Optica Applicata, Vol. XLIX, No. 3, 2019
DOI: 10.5277/oa190302

Spectroscopic properties of Er^{3+}-doped fluorotellurite glasses modified by Nb_2O_5 and WO_3

Bożena BURTAN-GWIZDAŁA[1*], Manuela REBEN[2], Jan CISOWSKI, El SAYED YOUSEF[3, 4], Radosław LISIECKI[5], Iwona GRELOWSKA[2]

[1] Institute of Physics, Cracow University of Technology, ul. Podchorążych 1, 30-084 Cracow, Poland

[2] Faculty of Materials Science and Ceramics, AGH – University of Science and Technology, al. Mickiewicza 30, 30-059 Cracow, Poland

[3] Department of Physics, Faculty of Sciences, King Khalid University, P.O. Box 9004, Abha, Saudi Arabia

[4] Research Center for Advanced Materials Science (RCAMS), King Khalid University, Abha 61413, P. O. Box 9004, Saudi Arabia

[5] Institute of Low Temperatures and Structure Research, Polish Academy of Sciences, ul. Okólna 2, 50 950 Wrocław, Poland

[*] Corresponding author: burtan_bozena@wp.pl

We have investigated the spectroscopic properties of Er^{3+}-doped fluorotellurite glasses with the basic molar composition 75%TeO_2–10%P_2O_5–10%ZnO–5%PbF_2, modified by replacing 5% TeO_2 by a metal oxide, namely WO_3 or Nb_2O_5. The absorption edge of the glasses studied has been described within the Urbach approach, while the absorption and photoluminescence spectra have been analyzed in terms of the standard Judd–Ofelt theory, along with the photoluminescence decay of the $^4I_{13/2}$ and $^4S_{3/2}$ levels of the Er^{3+} ion. The absorption and emission spectra of the $^4I_{15/2} \leftrightarrow {}^4I_{13/2}$ infrared transition have been analyzed within the McCumber theory to yield the peak emission cross-section and figure of merit for the amplifier gain. It appears that the fluorotellurite glass containing WO_3 as a modifier is characterized by the largest figure of merit, indicating this matrix as a promising new host for doping with Er^{3+} ions.

Keywords: fluorotellurite glasses, erbium ion, absorption, Judd–Ofelt analysis, photoluminescence, McCumber approach.

1. Introduction

Fluorotellurite glasses are promising materials for photonics applications. Of all oxide glasses, tellurite glasses are good candidates for infrared applications fiber optic laser materials due to the low phonon energy, high refractive index and wide transmission window [1–3].

In particular, Er^{3+}-doped tellurite glasses have been extensively studied due to their broadband infrared emission at 1.5 μm suitable for application in optical amplification and fiber lasers [4, 5].

In our previous studies [6], we tested the optical properties of fluorotellurite glasses of various compositions doped with erbium ions. It appears that the glass containing MgO as a modifier is characterized by the largest figures of merit (FOM) suggesting that such fluorotellurite matrix can be a good novel host for Er^{3+} ion doping. In this work we tested two other modifiers, namely Nb_2O_5 and WO_3.

2. Experiment

The basic fluorotellurite glass matrix used in this work consists of four components, namely $75TeO_2–10P_2O_5–10ZnO–5PbF_2$, in mol% (sample TPZP-Er in Table 1). Replacing 5 mol% of TeO_2 by the equivalent modifier amount, the glasses with composition $70TeO_2–10P_2O_5–10ZnO–5PbF_2–5M_xO_y$ have been obtained (see [7] for details), where the modifier $M_xO_y = WO_3$ or Nb_2O_5 (in Table 1, samples TPZPW-Er, TPZPNb-Er, respectively).

The densities, determined from the Archimedes law, and the resulting concentrations N of Er^{3+} ions in the glasses studied, are presented in Table 1.

T a b l e 1. Characteristics of fluorotellurite glasses doped with Er^{3+} ions.

Sample	Glass matrix composition [mol%]	Molar mass [g/mol]	Density [g/cm^3]	N [10^{19} cm^{-3}]
TPZPNb-Er	$70TeO_2–10P_2O_5–10ZnO–5PbF_2–5Nb_2O_5$	159.60	5.42	4.09
TPZPW-Er	$70TeO_2–10P_2O_5–10ZnO–5PbF_2–5WO_3$	157.90	5.34	4.02
TPZP-Er	$75TeO_2–10P_2O_5–10ZnO–5PbF_2$	154.29	5.26	3.97

For spectroscopic measurements, the glass samples were sliced and polished to dimensions of about $10 \times 10 \times 2$ mm^3. The transmission and reflection spectra were recorded with a PerkinElmer LAMBDA 900 spectrophotometer [8, 9].

The photoluminescence spectra were measured applying an Optron Dong Woo fluorometer system; the luminescence decay curves were measured following a short pulse excitation provided by an optical parametric oscillator pumped by a third harmonic of a Nd:YAG laser [8, 9]. All measurements were performed at room temperature.

3. Results and discussion

Using the transmittance and reflectance spectra, we have determined the dispersion of the absorption coefficient of the investigated fluorotellurite glasses doped with Er^{3+} ions (see Table 1), as presented in Fig. 1.

In general, the absorption spectra of the investigated samples are quite similar to each other, since there are only small differences in the glass composition and Er^{3+} ion concentration (see Table 1). However, looking at energies higher than 22000 cm^{-1} (2.78 eV), it can be seen that the absorption edge shifts by about 4000 cm^{-1}, when passing from

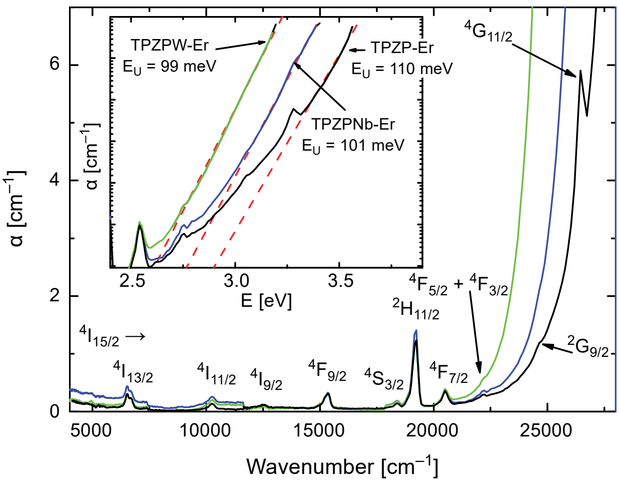

Fig. 1. Absorption spectra of Er^{3+}-doped fluorotellurite glass samples. Solid curves in the inset show the absorption coefficient *vs*. photon energy in the region of the Urbach absorption edge. Dotted curves represent the Urbach relation fitted to the experimental data above 3.36 eV, *i.e*. above the $^4I_{15/2} \rightarrow {^4G_{11/2}}$ absorption band of the Er^{3+} ion.

sample TPZPW-Er to sample TPZP-Er, that enables one to observe the $^4G_{11/2}$ peak for the latter sample.

In the near infrared (NIR), the absorption spectra consist of three bands, corresponding to the transitions $^4I_{15/2} \rightarrow {^4I_{13/2,\ 11/2,\ 9/2}}$. In the visible spectral range (VIS), there are further seven bands for sample TPZP-Er and five for samples TPZPNb-Er and TPZPW-Er.

At the photon energy above 3.36, 3.16 and 2.98 eV for samples TPZP-Er, TPZPNb-Er and TPZPW-Er, respectively, the absorption coefficient obeys the Urbach relation $\alpha \propto \exp(E/E_U)$ with E_U – the Urbach energy that is a measure of disorder. As

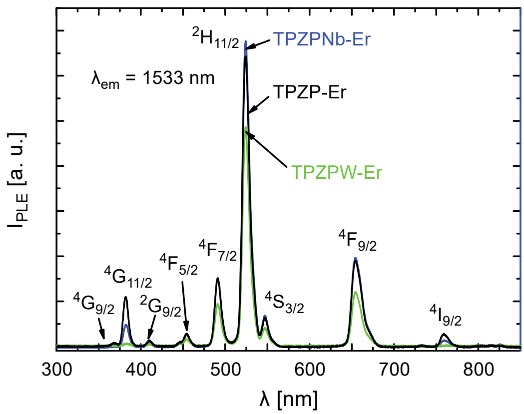

Fig. 2. Photoluminescence excitation (PLE) spectra of Er^{3+}-doped fluorotellurite glasses monitored at λ_{em} = 1533 nm.

seen in the inset, the Urbach energy for sample TPZP-Er is significantly higher than for other samples indicating that the former sample is more defected, *i.e.* is characterized by a higher glass network disorder.

The obtained absorption spectra of the studied glasses have been completed with the photoluminescence excitation (PLE) spectra that are shown in Fig. 2.

As can be seen in Fig. 2, the registration of PLE spectra has made it possible to observe for all samples, apart from levels present in the absorption spectra (Fig. 1), also the higher-lying level $^4G_{9/2}$; additionally, for samples TPZPNb-Er and TPZP-Er, the $^4G_{11/2}$ level, absent in the absorption spectrum, is seen in the PLE spectrum.

3.1. Judd–Ofelt analysis

In a further analysis, we have applied the standard Judd–Ofelt theory [9] to the observed absorption bands from Fig. 2; the experimental oscillator strengths for transitions from the ground $^4I_{15/2}$ level of Er^{3+} ion to consecutive excited levels have been determined by numerical integration of the corresponding absorption bands, subtracting the background absorption of the glass matrices.

Table 2 summarizes the experimental and calculated oscillator strengths of erbium ions in the studied glasses together with the phenomenological Judd–Ofelt parameters and root-mean square deviation. Values of the reduced matrix elements for particular electric-dipole transitions have been taken from [10]; as for the magnetic-dipole transitions, it concerns the $^4I_{15/2} \rightarrow {}^4I_{13/2}$ absorption band and this has been taken into account as the product of *n* and the oscillator strength in vacuum from [11].

The obtained values of Ω_t parameters for the studied samples are comparable with those found in other Er^{3+}-doped tellurite glasses and exhibit the same trend, namely

T a b l e 2. Measured and calculated oscillator strengths as well as Judd–Ofelt intensity parameters of Er^{3+} ions in fluorotellurite glasses.

Transition from $^4I_{15/2}$ to:	Energy [cm^{-1}]	Oscillator strength P (×10^{-6})					
		Sample TPZPNb-Er		Sample TPZPW-Er		Sample TPZP-Er	
		P_{exp}	P_{cal}	P_{exp}	P_{cal}	P_{exp}	P_{cal}
$^4I_{13/2}$	6580	1.54	1.85	2.46	2.11	2.05	1.81
$^4I_{11/2}$	10220	0.94	0.62	0.98	0.73	0.75	0.57
$^4I_{9/2}$	12510	0.60	0.39	0.45	0.55	0.38	0.50
$^4F_{9/2}$	15330	2.18	2.27	3.16	3.02	2.56	2.59
$^4S_{3/2}$	18340	0.40	0.48	0.49	0.57	0.36	0.43
$^2H_{11/2}$	19160	9.93	9.93	12.06	12.07	9.96	10.11
$^4F_{7/2}$	20430	2.29	2.10	2.26	2.62	2.22	2.08
Ω_2 (×10^{-20} cm^2)		4.20		5.13		3.61	
Ω_4 (×10^{-20} cm^2)		1.28		1.85		1.25	
Ω_6 (×10^{-20} cm^2)		0.82		1.01		0.77	
σ_{rms} (×10^{-6})		0.27		0.29		0.11	

$\Omega_2 > \Omega_4 > \Omega_6$ [12–15]. It can be also seen that the sample TPZPW-Er is characterized by the highest value of the Ω_6 parameter which has the decisive effect for enhancing the 1.5 μm band photoluminescence [16].

The determined Judd–Ofelt parameters have been used to estimate the total radiative lifetimes τ_{rad} of Er^{3+} excited states, and especially those of the ${}^4S_{3/2}$ and ${}^4I_{13/2}$ levels that can be compared with experimental data as presented below.

3.2. Emission spectra

Figure 3 shows the photoluminescence emission spectra of erbium-doped fluorotellurite glasses. To obtain the relative σ_{em} emission cross-section, the emission spectra were divided by the Er^{3+} ion concentration N.

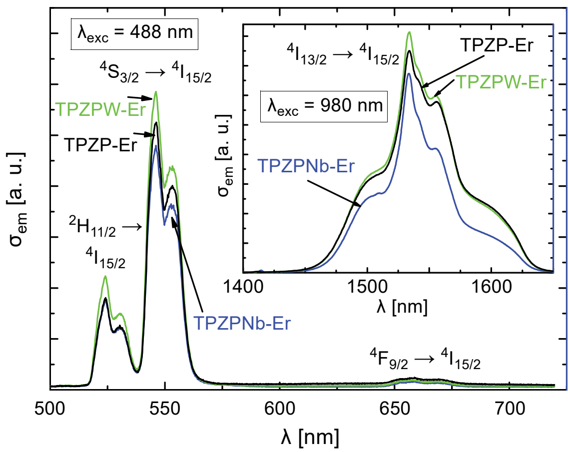

Fig. 3. Relative emission cross-section spectra of Er^{3+}-doped fluorotellurite glasses obtained in the visible and near-infrared regions under excitation at 488 and 980 nm, respectively.

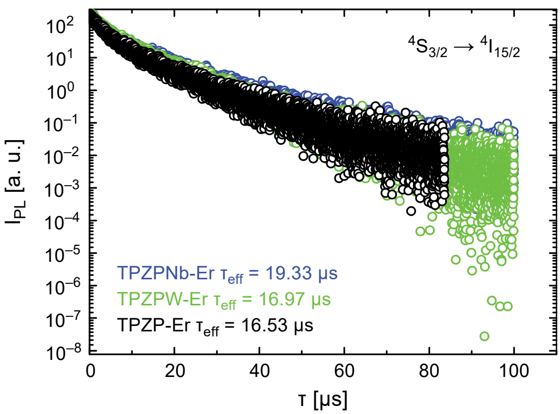

Fig. 4. Photoluminescence decay of the ${}^4S_{3/2}$ state of Er^{3+} ions for all samples.

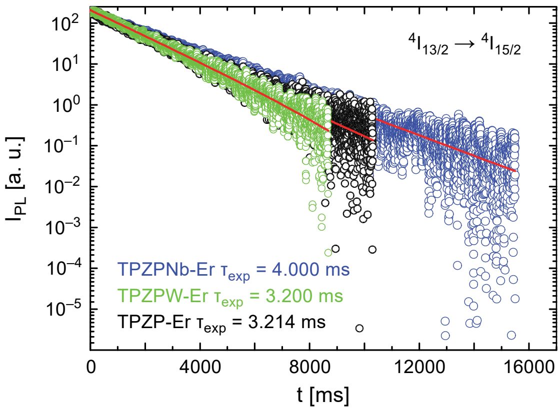

Fig. 5. Luminescence lifetimes of the $^4I_{13/2}$ state of Er^{3+} ions for all samples.

T a b l e 3. Lifetimes of the Er^{3+} emission bands in fluorotellurite glasses determined experimentally (τ_{exp} and τ_{eff}) and those calculated within the Judd–Ofelt approach (τ_{rad}) along with quantum efficiencies ($\eta = \tau_{exp}/\tau_{rad}$).

Sample	$^4I_{13/2}$ lifetime			$^4S_{3/2}$ lifetime		
	τ_{exp} [ms]	τ_{rad} [ms]	η [%]	τ_{eff} [μs]	τ_{rad} [μs]	η [%]
TPZPNb-Er	4.00	4.32	93	19.33	378	5.1
TPZPW-Er	3.20	3.95	81	16.97	327	5.2
TPZP-Er	3.21	4.36	74	16.53	397	4.2

Figure 3 shows two high-intensity emission bands attributed to the $^2H_{11/2} \rightarrow {}^4I_{15/2}$ and $^4S_{3/2} \rightarrow {}^4I_{15/2}$ transitions, and a much weaker one corresponding to the $^4F_{9/2} \rightarrow {}^4I_{15/2}$ transition; the inset presents the $^4I_{13/2} \rightarrow {}^4I_{15/2}$ emission in the NIR region.

The photoluminescence decays of $^4S_{3/2}$ and $^4I_{13/2}$ excited levels for all samples are shown in Figs. 4 and 5, respectively.

The $^4I_{13/2} \rightarrow {}^4I_{15/2}$ emission has an exponential character, while the $^4S_{3/2} \rightarrow {}^4I_{15/2}$ emission appears to be slightly non-exponential. For this reason, we have determined the effective lifetime defined as [17]

$$\tau_{\text{eff}} = \frac{\int t I(t) \mathrm{d}t}{\int I(t) \mathrm{d}t} \tag{1}$$

for this transition and in Table 3 we have gathered the experimental data for all investigated samples along with the radiative lifetimes τ_{rad} calculated within the Judd–Ofelt approach.

It appears that the quantum efficiency of the $^4I_{13/2} \rightarrow {}^4I_{15/2}$ transition is quite high, being the highest for sample TPZPNb-Er.

3.3. Absorption and emission cross-sections of $^4I_{15/2} \leftrightarrow {}^4I_{13/2}$ transition

In this subsection we concentrate on the absorption cross-section (ACS) and the emission cross-section (ECS) of the $^4I_{15/2} \leftrightarrow {}^4I_{13/2}$ transition that are fundamental parameters for the erbium-doped fiber amplifiers (EDFA) [17].

The ACS is defined as $\sigma = \alpha/N$ and is easily obtained from the absorption spectra shown in Fig. 1 after subtracting the monotonic background absorption of the glass matrices.

As for the $^4I_{13/2} \to {}^4I_{15/2}$ ECS, it is given in arbitrary units in the inset of Fig. 4. To scale these emission spectra, we have used the McCumber approach [18] leading to relation between ACS and ECS in the form [19]

$$\sigma_{\mathrm{em}}(\lambda) = \exp\left(\frac{\varepsilon}{kT}\right)\sigma_{\mathrm{abs}}(\lambda)\exp\left(-\frac{hc}{\lambda kT}\right) \tag{2}$$

where k is the Boltzmann constant, T is the temperature, h is the Planck constant and c is the light velocity; the quantity ε, the key parameter of this equation, may be treated as the mean transition energy between $^4I_{15/2}$ to $^4I_{13/2}$ levels and can be easily evaluated as the arithmetic average of the barycenter energies of absorption and emission spectra [6]. Making use of barycenter wavelengths gathered in Table 4, we have obtained the values of ε as being equal to 6539, 6523 and 6525 cm^{-1} for samples TPZPNb-Er, TPZPW-Er and TPZP-Er, respectively. Finally, the measured emission spectra have been scaled to have the same peak value as the ECS peak calculated from Eq. (2). Both ECS spectra along with the ACS spectrum for sample TPZP-Er, treated as an example, are shown in Fig. 6.

As is seen in Fig. 6, the McCumber curve reflects quite satisfactorily the shape of the measured ECS spectrum; some deviations, especially around the ECS maximum, are due to the neglect of broadening of the Stark components in deriving Eq. (2) [20, 21].

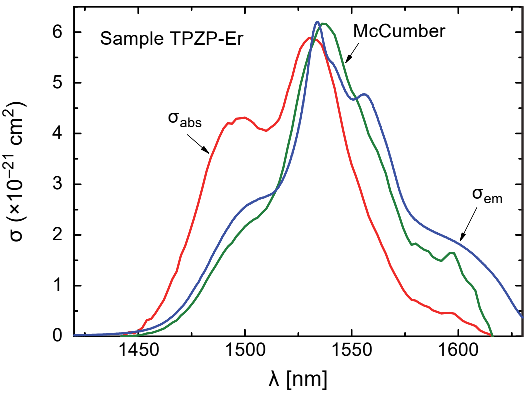

Fig. 6. Experimental ACS (σ_{abs}) and ECS spectra (σ_{em}) along with ECS spectrum calculated from McCumber Eq. (2) for sample TPZP-Er.

T a b l e 4. Peak wavelengths λ_p, barycenter wavelengths λ_b and effective linewidths $\Delta\lambda_{eff}$ of ${}^4I_{15/2} \leftrightarrow {}^4I_{13/2}$ transition as well as peak emission cross-sections σ^p_{em} and figures of merit (FOM) for amplifier gain for Er^{3+}-doped fluorotellurite glasses.

Sample	${}^4I_{15/2} \to {}^4I_{13/2}$ absorption			${}^4I_{13/2} \to {}^4I_{15/2}$ emission				
	λ_p [nm]	λ_b [nm]	$\Delta\lambda_{eff}$ [nm]	λ_p [nm]	λ_b [nm]	$\Delta\lambda_{eff}$ [nm]	σ^p_{em} [$\times 10^{-21}$ cm^2]	FOM [$\times 10^{-23}$ cm^{2}s]
TPZPNb-Er	1531.7	1518.6	63.3	1533.7	1540.3	58.9	5.59	2.24
TPZPW-Er	1534.3	1523.1	73.1	1534.2	1543.2	68.3	7.63	2.44
TPZP-Er	1531.3	1521.1	71.2	1533.9	1544.0	72.2	6.17	1.98

Taking into account the asymmetric shapes of both absorption and emission spectra, we have calculated the so-called effective linewidth $\Delta\lambda_{eff}$, instead of full-width at half-maximum (FWHM) [22]

$$\Delta\lambda_{eff} = \frac{1}{I_p}\int I(\lambda)\mathrm{d}\lambda \tag{3}$$

where I_p is the peak value of ACS or ECS.

The obtained effective linewidths as well as other parameters characterizing the ACS and ECS spectra are shown in Table 4 along with figures of merit (FOM) for the amplifier gain defined as the product of stimulated cross-section and experimental lifetime [23, 24]. Since efficiency of a fiber amplifier is proportional to FOM, therefore, as far as the material aspects are concerned, a large value of FOM is strongly desirable.

It can be seen from Table 4, that sample TPZPW-Er containing WO_3 is characterized by the largest FOM suggesting that a fluorotellurite glass matrix with this oxide as a modifier can be a good novel host for Er^{3+} ion doping.

4. Conclusions

The Urbach energy values E_U, determined in the region of the absorption edge, indicate that the glass without modifiers (sample TPZP-Er with $E_U = 110$ meV) is more defected in comparison to two other glasses containing modifiers, *i.e.* TPZPNb-Er (with $E_U = 101$ meV) and TPZPW-Er (with $E_U = 99$ meV).

Applying the standard Judd–Ofelt theory to the absorption spectra of the samples studied, the Judd–Ofelt intensity parameters Ω_2, Ω_4 and Ω_6 have been estimated, exhibiting the same trend, namely $\Omega_2 > \Omega_4 > \Omega_6$. It has been also found that the sample TPZPW-Er is characterized by the highest value of the Ω_6 parameter which has the decisive effect for enhancing the 1.5 μm band photoluminescence.

The absorption and emission cross-section results show that sample TPZPW-Er is characterized by the largest figure of merit for the amplifier gain.

The above-mentioned features of the Er^{3+}-doped fluorotellurite matrix, containing tungsten oxide as a modifier, suggest that such matrix may be, from the point of view of possible application in optoelectronics and telecommunication, a promising new host for doping with lathanide ions.

Acknowledgments – This work was supported by the statutory funds of AGH University of Science and Technology, Department of Materials Science and Ceramics AGH, number WIMiC No 11.11.160.365 in 2018, and by King Khalid University, the Ministry of Education and the Kingdom of Saudi Arabia with a grant (RCAMS/ KKU/1-17-4) under research center for advanced material science.

References

[1] Wang J.S., Vogel E.M., Snitzer E., *Tellurite glass: a new candidate for fiber devices*, Optical Materials **3**(3), 1994, pp. 187–203, DOI: 10.1016/0925-3467(94)90004-3.

[2] Richards B., Tsang Y., Binks D., Lousteau J., Jha A., *Efficient ~2 μm Tm^{3+}-doped tellurite fiber laser*, Optics Letters **33**(4), 2008, pp. 402–404, DOI: 10.1364/OL.33.000402.

[3] Mori A., Ohishi Y., Sudo S., *Erbium-doped tellurite glass fibre laser and amplifier*, Electronics Letters **33**(10), 1997, pp. 863, 864, DOI: 10.1049/el:19970585.

[4] Irannejad M., Fernandez T., Joshi P., Zhao Z., Lousteau J., Richards B., Jose G., Jha A., *Erbium -ion-doped tellurite glass fibers and waveguides—devices and future prospective: part II*, International Journal of Applied Glass Science **4**(3), 2013, pp. 202–213, DOI: 10.1111/ijag.12026.

[5] Narro-Garcia R., Desirena H., Chillcce E.F., Barbosa L.C., Rodriguez E., De la Rosa E., *Optical and spectroscopic characterization of Er^{3+}–Yb^{3+} co-doped tellurite glasses and fibers*, Optics Communications **317**, 2014, pp. 93–101, DOI: 10.1016/j.optcom.2013.11.056.

[6] Burtan-Gwizdała B., Reben M., Cisowski J., Grelowska I., El SayedYousef, Algarni H., Lisiecki R., Nosidlak N., *Spectroscopic properties of Er^{3+}-doped fluorotellurite glasses containing various modifiers*, Optical Materials **73**, 2017, pp. 509–516, DOI: 10.1016/j.optmat.2017.09.001.

[7] Reben M., El Sayed Yousef, Grelowska I., Kosmal M., Szumera M., *Influence of modifiers on the thermal characteristic of glasses of the TeO_2–P_2O_5–ZnO–PbF_2 system*, Journal of Thermal Analysis and Calorimetry **125**(3), 2016, pp. 1279–1286, DOI: 10.1007/s10973-016-5421-y.

[8] Burtan B., Cisowski J., Mazurak Z., Jarzabek B., Czaja M., Lisiecki R., Ryba-Romanowski W., Reben M., Grelowska I., *Concentration-dependent spectroscopic properties of Pr^{3+} ions in TeO_2–WO_3–PbO–La_2O_3 glass*, Journal of Non-Crystalline Solids **400**, 2014, pp. 21–26, DOI: 10.1016/j.jnoncrysol.2014.04.016.

[9] Burtan-Gwizdała B., Reben M., Cisowski J., Lisiecki R., Ryba-Romanowski W., Jarząbek B., ManΣzurak Z., Nosidlak N., Grelowska I., *The influence of Pr^{3+} content on luminescence and opvσtical behavior of TeO_2- WO_3-PbO-Lu_2O_3 glass*, Optical Materials **47**, 2015, pp. 231–236, DOI: 10.1016/j.optmat.2015.05.028.

[10] Kaminskii A.A., *Crystalline Lasers: Physical Processes and Operating Schemes*, CRC Press, Boca Baton, 1996, pp. 227–306.

[11] Dodson C.M., Zia R., *Magnetic dipole and electric quadrupole transitions in the trivalent lanthanide series: calculated emission rates and oscillator strengths*, Physical Review B **86**(12), 2012, article ID 125102, DOI: 10.1103/PhysRevB.86.125102.

[12] Babu P., Hyo Jin Seo, Kesavulu C.R., Kyoung Hyuk Jang, Jayasankar C.K., *Thermal and optical properties of Er^{3+}-doped oxyfluorotellurite glasses*, Journal of Luminescence **129**(5), 2009, pp. 444 –448, DOI: 10.1016/j.jlumin.2008.11.014.

[13] Balda R., Al-Saleh M., Miguel A., Fdez-Navarro J.M., Fernandez J., *Spectroscopy and frequency upconversion of Er^{3+} ions in fluorotellurite glasses*, Optical Materials **34**(2), 2011, pp. 481–486, DOI: 10.1016/j.optmat.2011.04.021.

[14] BILIR G., OZEN G., TATAR D., ÖVEÇOĞLU M.L., *Judd–Ofelt analysis and near infrared emission properties of the Er^{3+} ions in tellurite glasses containing WO_3 and CdO*, Optics Communications **284**(3), 2011, pp. 863–868, DOI: 10.1016/j.optcom.2010.09.087.

[15] MONTEIRO G., LI Y., SANTOS L.F., ALMEIDA R.M., *Optical and spectroscopic properties of rare earth -doped (80–x)TeO_2–xGO_2–10Nb_2O_5–10K_2O glasses*, Journal of Luminescence **134**, 2013, pp. 284 –296, DOI: 10.1016/j.jlumin.2012.08.031.

[16] HUANG B., ZHOU Y., YANG F., WU L., QI Y., LI J., *The 1.53 μm spectroscopic properties of Er^{3+}/Ce^{3+}/Yb^{3+} tri-doped tellurite glasses containing silver particles*, Optical Materials **51**, 2016, pp. 9 –17, DOI: 10.1016/j.optmat.2015.11.004.

[17] DUVERGER-ARFUSO C., BOULARD B., JESTIN Y., FERRARI M., CHIASERA A., *Influence of $PrCl_3$-PrF_3 on the optical and spectroscopic properties of fluorogallate and fluoro-gallo-indate glasses*, Optical Materials **28**(4), 2006, pp. 441–447, DOI: 10.1016/j.optmat.2005.04.004.

[18] MCCUMBER D.E., *Einstein relations connecting broadband emission and absorption spectra*, Physical Review **136**(4A), 1964, pp. A954–A957, DOI: 10.1103/PhysRev.136.A954.

[19] MINISCALCO W.J., QUIMBY R.S., *General procedure for the analysis of Er^{3+} cross sections*, Optics Letters **16**(4), 1991, pp. 258–260, DOI: 10.1364/OL.16.000258.

[20] HUANG C.-H., MCCAUGHAN L., GILL D.M., *Evaluation of absorption and emission cross sections of Er-doped $LiNbO_3$ for application to integrated optic amplifiers*, Journal of Lightwave Technology **12**(5), 1994, pp. 803–809, DOI: 10.1109/50.293972.

[21] QUIMBY R.S., *Range of validity of McCumber theory in relating absorption and emission cross sections*, Journal of Applied Physics **92**(1), 2002, pp. 180–187, DOI: 10.1063/1.1485112.

[22] WEBER M.J., ZIEGLER D.C., ANGELL C.A., *Tailoring stimulated emission cross sections of Nd^{3+} laser glass: observation of large cross sections for $BiCl_3$ glasses*, Journal of Applied Physics **53**(6), 1982, pp. 4344–4350, DOI: 10.1063/1.331214.

[23] WEI K., MACHEWIRTH D.P., WENZEL J., SNITZER E., SIGEL JR. G.H., *Pr^{3+}-doped Ge–Ga–S glasses for 1.3 μm optical fiber amplifiers*, Journal of Non-Crystalline Solids **182**(3), 1995, pp. 257–261, DOI: 10.1016/0022-3093(94)00513-3.

[24] FEIFEI HUANG, JIMENG CHENG, XUEQIANG LIU, LILI HU, DANPING CHEN, *Ho^{3+}/Er^{3+} doped fluoride glass sensitized by Ce^{3+} pumped by 1550 nm LD for efficient 2.0 μm laser applications*, Optics Express **22**(17), 2014, pp. 20924–20935, DOI: 10.1364/OE.22.020924.

Received November 14, 2018
in revised form January 25, 2019